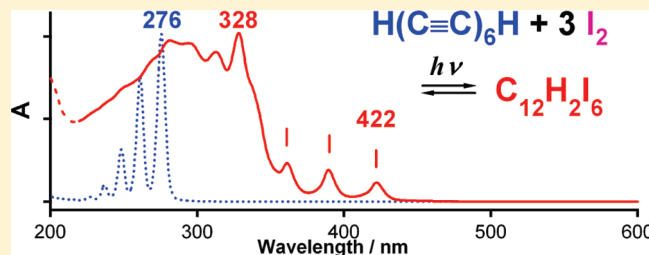


Photoinduced Reaction of Hydrogen-End-Capped Polyynes with Iodine Molecules

Yoriko Wada,[†] Tomonari Wakabayashi,^{*,†} and Tatsuhisa Kato[‡][†]Department of Chemistry, Kinki University, Higashi-Osaka 577-8502, Japan[‡]Institute for the Promotion of Excellence in Higher Education, Kyoto University, Kyoto 606-8501, Japan

ABSTRACT: Hydrogen-end-capped polyynes, $\text{H}(\text{C}\equiv\text{C})_n\text{H}$ ($n = 5-7$), were photoirradiated in the presence of iodine molecules in nonpolar solvents to find a dramatic change in the UV/vis absorption spectrum. Absorption bands of polyynes in the UV and the band of I_2 in the visible region disappeared, whereas weaker bands of polyynes were intensified in the near UV region. The emerging features are associated with vibronic bands in the symmetry-forbidden transition of the linear polyyne molecule. Stoichiometry for the reaction, i.e., $\text{C}_{12}\text{H}_2 + n\text{I}_2 \rightarrow \text{C}_{12}\text{H}_2\text{I}_{2n}$, was determined to be $n = 3$ from the concentration-dependence experiment. ^{13}C NMR spectra for 1:3 mixture of polyyne and iodine molecules, namely $\text{C}_{10}\text{H}_2/3\text{I}_2$ and $\text{C}_{12}\text{H}_2/3\text{I}_2$, exhibited five and six lines, respectively, all shifted to lower fields compared to those in the case without iodine. After removing excess I_2 by reductive reagent of Na_2SO_3 , recovery of the missing absorption bands for the components of C_{10}H_2 and I_2 was observed. These observations strongly support the formation of an unique molecular complex of $\text{C}_{2n}\text{H}_2\text{I}_6$ ($n = 5-7$) upon photoabsorption by an I_2 molecule within a cluster of polyyne and iodine molecules, $\text{C}_{2n}\text{H}_2(\text{I}_2)_m$ ($m \geq 3$).



1. INTRODUCTION

Hydrogen-end-capped polyyne, $\text{H}(\text{C}\equiv\text{C})_n\text{H}$ ($n \geq 2$), is one of the simplest model compounds for the system of sp-hybridized carbon chains. Conjugate π -electron system of sp-carbon materials is a promise for electronic conductivity¹ and nonlinear optical response.² Along with recent developments in the synthetic approach,³ polyynes stabilized by bulky end-capping groups have been investigated extensively,⁴⁻⁶ to reveal reduction in bond-length alternation for longer polyynes.⁶ Polyynes terminated by aromatic groups have been studied in view of the electronic structure.^{7,8} One of the ultimate goals of this stream is to form a novel carbon allotrope of well-defined crystalline structure.^{9,10} Attempts have been made to characterize aggregates of carbon clusters, C_m , to recognize fragility and reactivity of sp-hybridized carbon moieties embedded in the all-carbon materials.^{11,12} The title molecules of hydrogen-end-capped polyynes constituted of an ideally minimal molecular frame for supporting its π -electron system are stable enough in ambient conditions.

Recently, polyyne molecules were produced by laser ablation¹³ and by contact arc¹⁴ in liquids and the detection of longer polyynes was extended to C_{26}H_2 .¹⁵ By liquid-phase laser ablation, quantity of polyynes available in size-selective manner has been increased to a milligram order for C_{2n}H_2 ($n = 4-6$).¹⁶⁻¹⁸ Using size-separated polyynes, C_{2n}H_2 ($n = 4-8$), characterization was performed by normal Raman and SERS¹⁶ and resonance Raman spectroscopy.¹⁷ New optical emission spectra were detected for C_{2n}H_2 ($n = 5-8$) in the visible region by laser-induced emission spectroscopy in solutions.¹⁸

Stabilization of sp-carbon chain molecules into solid forms is crucial for exploiting optical properties of the one-dimensional π -electron system. Hydrogen-end-capped polyynes were trapped inside single-wall carbon nanotubes (SWNT) forming $\text{C}_{10}\text{H}_2@\text{SWNT}$ and demonstrated to be stable well above 300 °C.^{19,20} Optical response was investigated thoroughly by resonance Raman spectroscopy.^{21,22} The approach for stabilization of polyynes in SWNT was extended to five polyynes, $\text{C}_{2n}\text{H}_2@\text{SWNT}$ ($n = 4-8$).²³

Variation in color of iodine solutions has long been a subject in chemistry. The change in color was associated with the formation of molecular complexes of iodine molecules with aromatic hydrocarbons such as benzene.²⁴ Molecular structure of such a complex, e.g., I_2 -benzene, has been discussed along with ultrafast reaction dynamics via the photoexcited charge-transfer state.²⁵⁻²⁷ If we restrict our attention to stable forms of iodine itself, we notice that there is a variety of chemical forms depending on the experimental conditions. Iodine exists mostly as I_2 molecules in nonpolar solvents such as in hexane, while, at least partly, as I_3^- anion in polar solvents such as in water. Both forms are in a closed-shell electronic structure and exhibit different colors in solutions, i.e., rose to purple for I_2 and yellow to brown for I_3^- depending on their concentrations. The anionic triiodide, I_3^- , is believed to be unstable in nonpolar solvents. However, it may be possible to exist in a dimeric form under the

Received: April 2, 2011

Revised: May 29, 2011

Published: May 31, 2011

presence of an appropriate donor specie in-between, forming a totally neutral, closed-shell molecular complex of the form of I_3 -D- I_3 . Such a complex, if it exists, can be an important precursor or intermediate in the process of widely accepted, versatile reactions such as substitution for saturated hydrocarbons and addition for unsaturated hydrocarbons conducted in nonpolar solvents. Our experimental finding presented in this work provides the first example of the formation of such an intermediate or byproduct in the reaction of iodine and polyynes under illumination of visible light.

We herein report our observation of spectral changes in the UV/vis absorption spectra for mixtures of size-separated polyynes and iodine molecules in nonpolar solvents. Stoichiometry for the complex-forming reaction was determined experimentally. Molecular structure was investigated by NMR spectroscopy. Formation mechanism of the polyne-iodine complex in the photoinduced reaction is discussed along with symmetry considerations on the electronic transitions for the series of polyne molecules, $C_{2n}H_2$ ($n = 5-7$).

2. EXPERIMENTS

Polyynes were produced by laser ablation of carbon particles (graphite >99%) suspended in hexane (*n*-hexane >95%) using a Q-switched Nd:YAG laser system (532 nm, 0.4 J pulse⁻¹, 10 Hz). Irradiation with unfocused laser pulses typically for 5 h (1.8×10^5 pulses) resulted in the formation of polyynes of various sizes, $C_{2n}H_2$ ($n = 4-8$).^{16-20,23} After filtration, the solution was concentrated then subjected to high performance liquid chromatography (HPLC) for separation and purification, using a polymeric octadecyl silica (ODS) column eluted with hexane (SC18AR $\phi 10 \times 250$ mm, 4 mL min⁻¹).¹⁶

Polyne-iodine complex was prepared in the dark by mixing a solution of size-separated polyne molecules ($\sim 10^{-6}$ mol L⁻¹ in hexane) and a solution containing an excess amount of iodine in hexane. Commercially available iodine was used without further purification (Wako Pure Chemical Industries, Ltd. I_2 >99.8%). The mixture was irradiated with visible light of a fluorescent tube for several minutes. In order to remove residual I_2 molecules, the solution was treated with an aqueous solution of sodium sulfite (Kishida Chameleon Reagent Na_2SO_3 >97%) and the hexane phase was investigated by UV/vis absorption spectroscopy. Absorption spectra were recorded in the region of 200–600 nm on a spectrophotometer (JASCO V-670, 0.5 nm resolution).

The effect of visible light on the formation of polyne-iodine complexes was studied in detail. A solution containing $C_{10}H_2$ and I_2 in hexane was prepared in the dark. Absorption spectra were measured every 10 min of either a dark or a bright period of illumination. It was confirmed that, only under the condition of the bright period of illumination, the reaction proceeded showing an exponential decay in the absorption band at 252 nm for $C_{10}H_2$. Spectral profile of the light tube (Osram FPL27EXN BB-1) used throughout the experiments was measured by a spectrophotometer (Ocean Optics USB2000). The light emitted from the tube spans from 320 to 720 nm, comprising several major bands peaking at 405, 436, 489, 546, 588, and 612 nm. Experiments of band-selective irradiation revealed that irradiation with the latter three bands, i.e., 546, 588, and 612 nm, provided comparable effects in the decay for $C_{10}H_2$. The spectral region for the emission from the light tube

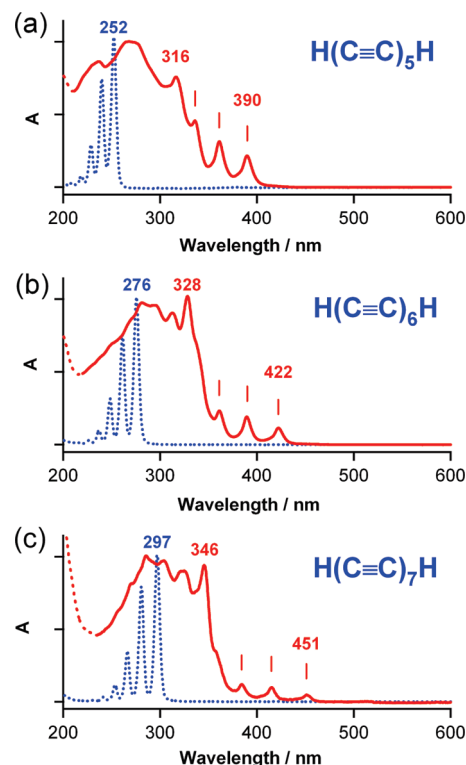


Figure 1. UV/vis absorption spectra for hydrogen-end-capped polyynes in hexane by dotted lines in blue (a) $C_{10}H_2$, (b) $C_{12}H_2$, and (c) $C_{14}H_2$ and for polyne-iodine complexes in hexane by solid lines in red (a) $C_{10}H_2I_6$, (b) $C_{12}H_2I_6$, and (c) $C_{14}H_2I_6$.

coincided with that for a broad electronic absorption band of iodine molecule in hexane, 520 ± 80 nm.²⁴

For higher sensitivity in ^{13}C NMR spectroscopy, isotope-enriched carbon powder ($^{13}C \sim 10\%$) was used for production of polyynes by laser ablation. Following separation and purification of $C_{10}H_2$ by HPLC, the solvent of hexane was replaced by 1,1,2,2-tetrachloroethane- d_2 (TCE- d_2 >99.6%) without completely being dried in order for $C_{10}H_2$ not to polymerize. For the NMR measurement of a polyne-iodine system, a solution of I_2 in TCE- d_2 was added to the solution of $C_{10}H_2$ in TCE- d_2 under the condition of ambient light. The 1H and ^{13}C NMR spectra were recorded on a spectrometer (JEOL JNM-ECA500, 500 MHz for 1H). Similarly to $C_{10}H_2$, 1H and ^{13}C NMR spectra were measured for $C_{12}H_2$. Spin-spin coupling constants, J_{CH} , for $C_{10}H_2$ and $C_{12}H_2$ were also measured for conditions with and without I_2 .

3. RESULTS AND DISCUSSION

3.1. Spectral Changes. Hydrogen-end-capped polyynes are identified by their UV absorption spectra in solutions, $\epsilon \sim 10^5$ cm⁻¹ mol⁻¹ L, showing a characteristic vibrational progression of bands with an increment of ~ 2000 cm⁻¹.^{28,29} In Figure 1, UV absorption spectra for the series of polyynes are shown by dotted lines in blue. The leading peak for each polyne in hexane is seen at 252 nm for $C_{10}H_2$ in panel a, 276 nm for $C_{12}H_2$ in panel b, and 297 nm for $C_{14}H_2$ in panel c, exhibiting a systematic shift to longer wavelength proportionally to the size of the π -electron system.

The absorption spectra for the solution of polyne molecules in hexane dramatically changed upon addition of a solution of

Table 1. UV/vis Absorption Bands in nm for Polyynes and Iodine Complexes

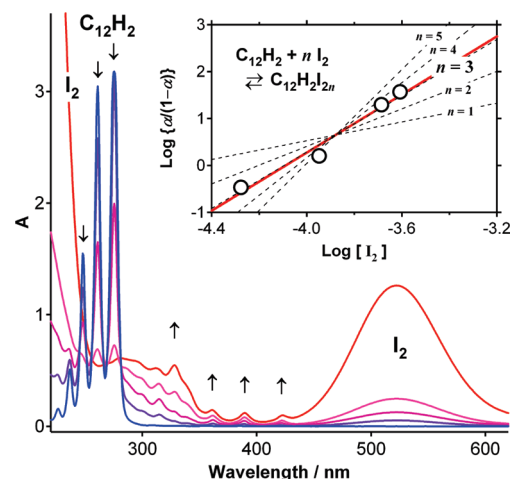
transition	C ₁₀ H ₂	C ₁₀ H ₂ I ₆	C ₁₂ H ₂	C ₁₂ H ₂ I ₆	C ₁₄ H ₂	C ₁₄ H ₂ I ₆
1 ¹ Δ _u ← X ¹ Σ _g ⁺	384 ^{a,b} 357 ^{a,b} 333 ^{a,b} 312 ^{a,b}	390 ^d 361 ^d 336 ^d 316 ^d	418 ^b 385 ^b 358 ^b	422 ^d 390 ^d 361 ^d 328 ^d 312 ^d	445 ^b 411 ^b 380 ^b 355 ^b	451 ^d 415 ^d 384 ^d 346 ^d
2 ¹ Δ _u ← X ¹ Σ _g ⁺						
1 ¹ Σ _u ⁺ ← X ¹ Σ _g ⁺	252 ^c 239 ^c 228 ^c		276 ^c 261 ^c 248 ^c		297 ^c 281 ^c 266 ^c	

^a Reference 30. ^b Reference 18. ^c Reference 28. ^d This work.

hexane that contained an excess quantity of I₂ molecules. In Figure 1, the spectra are shown by solid lines in red. Before the measurement of the spectra, residual iodine molecules were removed from hexane phase to aqueous phase by addition of aqueous solution containing reductive reagent of Na₂SO₃.

Figure 1a shows UV/vis absorption spectra for the system of C₁₀H₂ and I₂ in hexane (solid line in red). The series of bands for intact C₁₀H₂ peaking at 252, 239, and 228 nm (dotted line in blue) disappeared, and new absorption features appeared in longer wavelengths. Among the newly appearing features, conspicuous bands are the band at 316 nm in the UV and those at 336, 361, and 390 nm in the near UV. The latter three bands with characteristic increments of ~2060 cm⁻¹ are associated with weak absorption bands observed for intact C₁₀H₂ as reported in the literature, namely absorption bands peaking at 333, 357, and 384 nm for C₁₀H₂ in hexane.^{18,30,31} The bands in the near-UV region observed in the present work are red-shifted slightly by 3–6 nm (270–400 cm⁻¹). The spectral position as well as vibrational pattern for C₁₀H₂ with iodine does not differ very much from that without iodine. This observation indicates that the electronic level structure of C₁₀H₂ is restored even after the reaction with iodine. The dramatic change in the appearance of the UV absorption spectra is primarily due to changes in strengths for the relevant electronic transitions of the C₁₀H₂ molecule.

For C₁₂H₂ and C₁₄H₂ also, spectral changes were observed as in the case for C₁₀H₂. The solid lines in red in panels b and c in Figure 1 show UV/vis absorption spectra after mixing with I₂ in hexane for C₁₂H₂ and C₁₄H₂, respectively. The spectra were recorded after removal of residual I₂ with excess Na₂SO₃. The UV absorption bands for intact C₁₂H₂ and C₁₄H₂ disappeared, and new absorption features emerged. Spectral pattern for the new features is analogous to the case for C₁₀H₂, i.e., a few peaks in the UV and three peaks with a separation of ~2000 ± 40 cm⁻¹ in longer wavelengths. The new band in the UV is peaking at 328 nm for C₁₂H₂ in panel b and 346 nm for C₁₄H₂ in panel c. For the series of bands in longer wavelengths, peak positions extend from near-UV to visible regions, i.e., 361, 390, and 422 nm for C₁₂H₂ in panel b and 384, 415, and 451 nm for C₁₄H₂ in panel c, which coincide well with those reported for weak absorption features for intact polyynes of C₁₂H₂ and C₁₄H₂ in hexane, within a few hundreds of wavenumbers.¹⁸ Coincidence in the spectral position, thus in the band origin and vibrational frequency, indicates again that the conjugated carbon chain of the intact polyyne molecule is retained after the reaction with iodine. The absorption bands observed for three polyynes before and after the treatment with iodine are summarized in Table 1.

**Figure 2.** Concentration dependence in the UV/vis absorption spectra for C₁₂H₂/I₂ system. Inset shows a plot for the complex-to-free ratio as a function of I₂ concentration. From the slope of the plot, stoichiometry for the reaction, C₁₂H₂ + *n* I₂ → C₁₂H₂I_{2*n*}, is determined to be *n* = 3.

3.2. Stoichiometry. In order to get insight into the reaction mechanism for the formation of the polyyne–iodine system, concentration dependence was investigated in more detail. Figure 2 shows UV/vis absorption spectra for a series of mixtures of C₁₂H₂ and I₂ in hexane with different I₂ concentrations, namely 0, ~4, ~8, ~16, and ~80 mol equiv to C₁₂H₂ polyyne. By increasing the concentration of iodine, the intensity for the band at 276 nm for C₁₂H₂ diminished, and the absorption features in-between 350 and 430 nm were intensified.

The following equilibrium is assumed in order to model the change in absorption intensity observed for the concentration dependence experiments in Figure 2.



The constant, *K*, is defined and parametrized as follows:

$$K = \frac{[\text{C}_{12}\text{H}_2\text{I}_{2n}]}{[\text{C}_{12}\text{H}_2][\text{I}_2]^n} = \frac{C\alpha}{C(1-\alpha)(d-nC\alpha)^n} \quad (2)$$

where *C* and *d* denotes initial concentrations for C₁₂H₂ and I₂, respectively. The extent of reaction, *α*, represents the fraction of polyyne molecules which reacted with iodine. The value of *α* can be evaluated from depletion in the absorption band for C₁₂H₂ in Figure 2. In the case that the intensity for the absorption band at 276 nm was saturated, one of the adjacent members in the vibrational progression at 261 or 248 nm was used for evaluation of *α*. Knowing the absorption coefficient at 520 nm for I₂ in hexane being *ε* = 9.2 × 10² cm⁻¹ mol⁻¹ L,²⁴ the concentration of I₂ in the equilibrium was evaluated from absorption intensity at 520 nm in Figure 2. For these wavelengths, 276, 261, and 248 nm for C₁₂H₂ and 520 nm for I₂, spectral impurity can be minimized since the relevant absorption features are disappearing upon the reaction (see Figure 1b), allowing one to make spectral decomposition.

Equation 2 is transformed into a linear equation with respect to logarithm of concentration for iodine, [I₂] = *d* − *nCα*.

$$\log \frac{\alpha}{1-\alpha} = \log K + n \log [\text{I}_2] \quad (3)$$

The inset in Figure 2 depicts a plot of figures evaluated for selected traces in the main panel of Figure 2, i.e., a plot of log

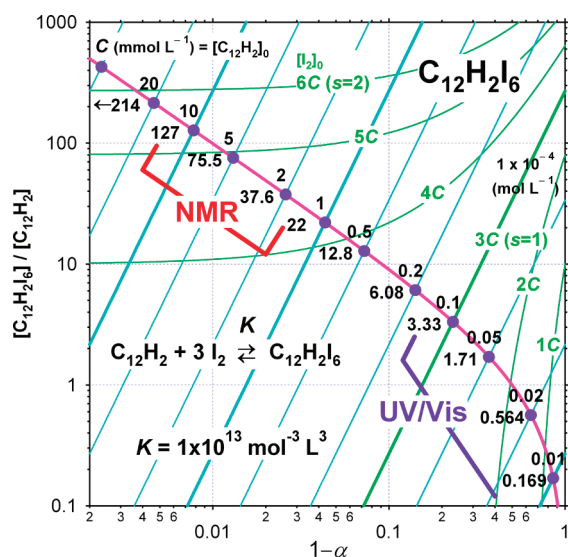


Figure 3. Calculated equilibrium fraction, $[C_{12}H_2I_6]/[C_{12}H_2]$, i.e., the complex-to-free ratio, $\alpha/(1 - \alpha)$, as a function of fraction for free $C_{12}H_2$, $1 - \alpha$, for the reaction of $C_{12}H_2 + 3I_2 \rightarrow C_{12}H_2I_6$. The experimentally estimated constant, $K = 1 \times 10^{13} \text{ mol}^{-3} \text{ L}^3$, was assumed. The fraction increases as the concentration of $C_{12}H_2$ increases from lower right to upper left (for detail, see text in section 3.3).

$\{\alpha/(1 - \alpha)\}$ as a function of $\log [I_2]$. From the slope of the plot, best-fit integer was determined to be $n = 3$. This stoichiometry means that one polyne molecule, $C_{12}H_2$, reacts with three I_2 molecules.

3.3. Fraction of $C_{12}H_2I_6$ and Its Concentration Dependence. The analysis presented above provided a constant K on the order of $\sim 10^{13} \text{ mol}^{-3} \text{ L}^3$. By using this constant $K = 1 \times 10^{13} \text{ mol}^{-3} \text{ L}^3$ and by adopting $n = 3$ in eq 2, the equilibrium fraction, i.e., the complex-to-free ratio, $[C_{12}H_2I_6]/[C_{12}H_2]$, can be calculated for a wide range of concentrations.

$$\frac{[C_{12}H_2I_6]}{[C_{12}H_2]} = \frac{\alpha}{1 - \alpha} = 27KC^3(s - \alpha)^3 \quad (4)$$

where the initial concentration of I_2 is represented by $d = 3sC$, with s being a factor in the unit of three-times molar equivalent to the initial concentration, C , for $C_{12}H_2$. In Figure 3, the thick curve in magenta plots the complex-to-free ratio, $\alpha/(1 - \alpha)$, as a function of the fraction for free $C_{12}H_2$, $1 - \alpha$. The parallel lines of slope 3 in light blue represent contours for 1:3 mixtures of $C_{12}H_2$ and I_2 ($s = 1$) for various initial concentrations, C , for $C_{12}H_2$. The group of curves in green converging upper right represents a variation in the case of other molar equivalents of I_2 ($s = 0.33-2$) in a specific case for the initial concentration, $C = 1 \times 10^{-4} \text{ mol L}^{-1}$, for $C_{12}H_2$.

In Figure 3, a point in the upper left corresponds to a high-concentration condition and that in the lower right to a low-concentration condition. The ordinate for the crossing point of the thick curve and one of the inclined lines gives the complex-to-free ratio at the equilibrium. At higher concentration, equilibrium moves to the complex-forming right-hand-side of eq 1, due to the third-order dependence. In the lower right in Figure 3, typical condition corresponding to UV/vis absorption spectroscopy is indicated, where the complex-to-free ratio for a 1:3 mixture of $C_{12}H_2$ and I_2 ($s = 1$) ranges on the order of unity, i.e., 0.17–3.33. The complex $C_{12}H_2I_6$ and free $C_{12}H_2$ are

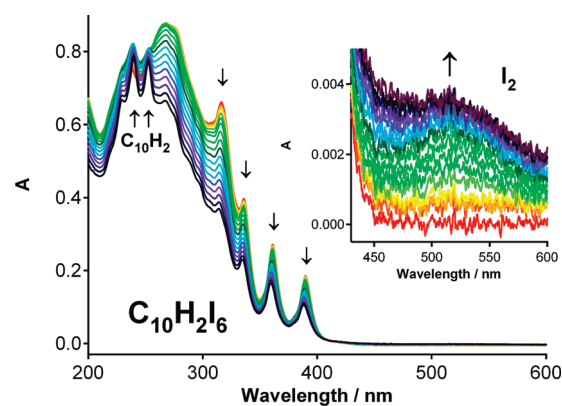


Figure 4. Recovery of free $C_{10}H_2$ and free I_2 (inset) from the complex $C_{10}H_2I_6$ upon illumination with visible light to a solution of the complex.

coexisting in comparable amounts to each other. In contrast to the relatively dilute conditions for UV/vis absorption spectroscopy, conditions for NMR spectroscopy are on orders-of-magnitude higher concentration. In the upper left in Figure 3, a typical condition corresponding to NMR spectroscopy is indicated, where the complex-to-free ratio for a 1:3 mixture of $C_{12}H_2$ and I_2 ($s = 1$) increases to 22–127. More than >95% of $C_{12}H_2$ molecules are existing in the form of the complex of $C_{12}H_2I_6$. The experimental results on the NMR spectroscopy are described in section 3.5.

Under the condition of an excess of I_2 relative to $C_{12}H_2$ ($s > 1$), the complex-to-free ratio can reach a value of $>10^2$ even under a dilute condition of low C , as indicated by a green curve in the upper left in Figure 3. Indeed, solutions for the measurement of the spectra in Figure 1 were prepared under such conditions, i.e., concentrations for I_2 in one-order higher relative to $\sim 10^{-5} \text{ mol L}^{-1}$ for polyynes. As a result, no trace of absorption features for free polyne molecules was discernible in the solid line spectra in red in Figure 1. This observation is compatible with considerations on the equilibrium. Concerning a further detail on the spectra in Figure 1, it should be noted that the residual I_2 had been removed prior to the measurement of the UV/vis absorption spectra. Therefore, for the moment of measurement, one has to consider the condition of a 1:3 mixture ($s = 1$), where a certain fraction of free polyne molecules is to be observed as tracing back to a point in the lower right in Figure 3. A key for understanding the discrepancy is the reaction barrier. Here we recall that the complex-forming reaction requires photoabsorption. It is natural to consider that the backward reaction also needs photoabsorption in order to initiate it.

3.4. Recovery of $C_{10}H_2$ and I_2 from the Complex $C_{10}H_2I_6$. Aiming at observation of the recovery of polyne molecules from the polyne–iodine complex, the solution of $C_{10}H_2I_6$ in hexane after removal of residual I_2 was irradiated with visible light. Figure 4 shows a series of UV/vis absorption spectra recorded redundantly after every 30 min irradiation for a total ~ 4.5 h. The bands for free $C_{10}H_2$ peaking at 252 and 239 nm emerged as the irradiation time increased. The intensity of the broad band for I_2 at 520 nm also increased as shown in the inset in Figure 4. Concomitantly, absorption bands in the near-UV region for the complex $C_{10}H_2I_6$ diminished in intensity. These observations clearly show that the reaction in eq 1 is reversible, at least to a certain fraction, under an appropriate condition with illumination with visible light.

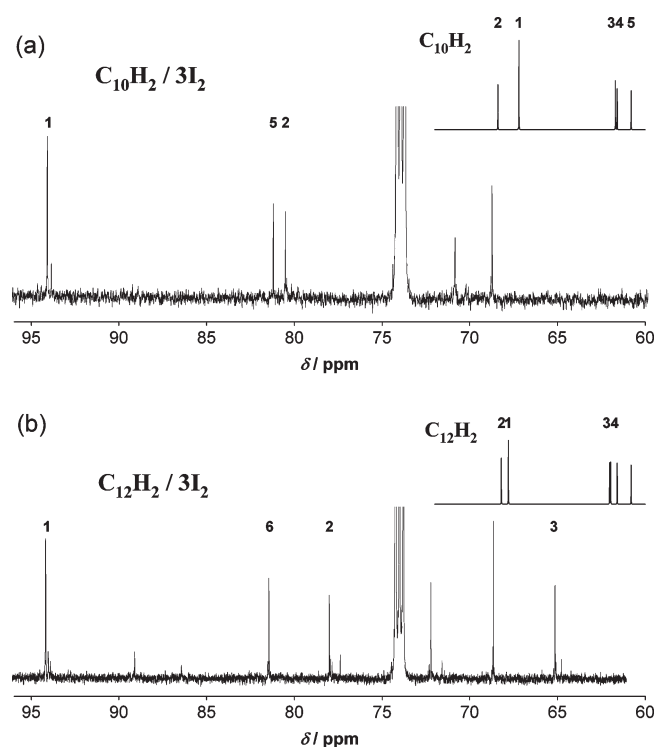


Figure 5. ^{13}C NMR spectra for polyynes, (a) C_{10}H_2 and (b) C_{12}H_2 , in 1,1,2,2-tetrachloroethylene- d_2 (peaks at 74 ppm). For sensitivity, ^{13}C -enriched carbon powder, $\sim 10\%$, was used for preparation of polyynes by laser ablation. Insets show ^{13}C NMR spectra for polyynes, (a) C_{10}H_2 and (b) C_{12}H_2 .

3.5. ^1H and ^{13}C NMR Spectra for $\text{C}_{10}\text{H}_2\text{I}_6$ and $\text{C}_{12}\text{H}_2\text{I}_6$

Figure 5a shows ^{13}C NMR spectrum for the mixture of C_{10}H_2 and its three-times molar equivalent of I_2 in TCE- d_2 , namely $\text{C}_{10}\text{H}_2/3\text{I}_2$. The spectrum for the system of $\text{C}_{10}\text{H}_2/3\text{I}_2$ clearly shows five lines within a range of 69–94 ppm. These lines are all shifted to lower fields compared to the five lines for the intact C_{10}H_2 in TCE- d_2 as shown by a stick spectrum in the inset in Figure 5a.¹⁷ In Table 2, chemical shifts, δ , in ^1H and ^{13}C NMR and coupling constants, J_{CH} , for the complex $\text{C}_{10}\text{H}_2\text{I}_6$ are compared with those for free C_{10}H_2 . The magnitude for splitting in J_{CH} was considerably reduced upon transformation from the intact polyne, C_{10}H_2 , to the complex, $\text{C}_{10}\text{H}_2\text{I}_6$, i.e., from 261 to 200 Hz for C1/C1', 51.4 to 12.5 Hz for C2/C2', and 7.1 to 0.5 Hz for C3/C3' for the sequence of H1-C1-C2-C3-C4-C5-C5'-C4'-C3'-C2'-C1'-H1'. The low-field shift for all the five lines indicates that magnetic shielding is weakened for all carbon nuclei for the complex, $\text{C}_{10}\text{H}_2\text{I}_6$.

The observed chemical shift at the lowest-field line is 94.0 ppm for C1/C1'. One might consider substitution of an end-capping hydrogen atom with an iodine atom. However, since the substitution could provide a significantly high-field line for ^{13}C in $\text{I}-\text{C}\equiv$ at <20 ppm,³² it is not compatible with our observation. Moreover, addition of iodine atoms to unsaturated triple bonds forming sp^2 -carbon structures could not be the case, because the observed line does not fall within the region for ethylenic carbon in >120 ppm.³³ Furthermore, the observed line is still close to the region for acetylenic carbon, even closer than the line for ^{13}C in $\text{N}\equiv\text{C}-$ at ~ 105 ppm.³⁴ The other lines observed in the present work fall well within a range for acetylenic sp carbon. The polyne-iodine complex in the present work is neither a substitution nor an addition product of iodine atoms.

Table 2. ^{13}C and ^1H NMR Chemical Shifts δ and Spin–Spin Coupling Constants J_{CH} for Polyynes C_{2n}H_2 and Iodine Complex $\text{C}_{2n}\text{H}_2\text{I}_6$ for $n = 5$ and 6 in 1,1,2,2-Tetrachloroethane- d_2

molecule	δ , ppm	J_{CH} , Hz	assignment
$\text{C}_{10}\text{H}_2^a$	68.4	51.4	C2
	67.2	261.4	C1
	61.7	7.1	C3
	61.6	1.7	C4
	60.8	0.0	C5
	2.12		H1
$\text{C}_{10}\text{H}_2\text{I}_6^b$	94.0	199.9	C1
	81.2	0.0	C5
	80.5	12.5	C2
	70.9	0.5	C3,C4
	68.8	0.5	C3,C4
	7.64		H1
$\text{C}_{12}\text{H}_2^a$	68.2	51.5	C2
	67.8	262.2	C1
	62.0	6.8	C3
	62.0	2.1	C4
	61.6	0.0	C5,C6
	60.8	0.0	C5,C6
$\text{C}_{12}\text{H}_2\text{I}_6^b$	2.16		H1
	94.1	199.6	C1
	81.4	0.0	C6
	78.0	12.7	C2
	72.2	0.0	C4,C5
	68.7	0.0	C4,C5
	65.2	0.8	C3
	7.66		H1

^a Reference 17. ^b This work.

Under the restriction by the stoichiometry of $n = 3$ for the reaction of $\text{C}_{10}\text{H}_2 + n \text{I}_2$ as described in section 3.2, the chemical composition for the product must be $\text{C}_{10}\text{H}_2\text{I}_6$. Moreover, from the NMR spectra in Figure 5a, a majority of products must have a unique structure for which the symmetric center is restored. One might still consider addition of iodine atoms to unsaturated $-\text{C}\equiv\text{C}-$ bonds in C_{10}H_2 . For $\text{C}_{10}\text{H}_2\text{I}_6$, it might be possible to conceive of a symmetric adduct, 1,2,5,6,9,10-hexaiodo-1,5,9-triene-3,7-diyne. It is easier to conceive of such symmetric adducts of six iodine atoms for polyynes with an odd-number of triple bonds, namely the series of $\text{C}_{4n+2}\text{H}_2$, which has a triple bond at the center of symmetry. On the other hand, for polyynes with an even-number of triple bonds, namely the series of C_{4n}H_2 , having a single bond at the center of symmetry, it is rather difficult to consider a symmetric adduct of six iodine atoms in a stable form. Otherwise the product must carry unstable cumulenyl bonds or free radicals along its carbon skeleton.

Figure 5b shows ^{13}C NMR spectrum for the mixture of C_{12}H_2 and its three-times molar equivalent of I_2 in TCE- d_2 , namely $\text{C}_{12}\text{H}_2/3\text{I}_2$. The observation of six lines, all shifted to lower fields compared to those for intact C_{12}H_2 in TCE- d_2 as shown in the inset in Figure 5b, provides again a restriction for the molecular structure of the product. A symmetric center, at least a 2-fold symmetry axis, C_2 , must be retained also for the complex, $\text{C}_{12}\text{H}_2\text{I}_6$.

3.6. Molecular Structure and Formation Mechanism of $C_{2n}H_2I_6$. For considerations on the molecular structure for polyyne-iodine complexes, we performed molecular orbital calculations at B3LYP/STO-3G density functional theory,³⁵ to find an energy minimum with a point group symmetry of C_2 for $C_{10}H_2I_6$. The six iodine atoms settled at equatorial positions of the molecular axis of $C_{10}H_2$ in the form of a skewed hexagonal ring, rather looking like two bent- I_3 units facing to the center of the polyynic carbon chain. The energy minimum for the complex, $C_{10}H_2I_6$, was at 2.37 eV above the ground state for the reactant system, $C_{10}H_2 + 3I_2$, and lower in energy than calculated dissociation energy of 2.42 eV for I_2 . These figures are fairly compatible with our experimental finding that the excitation is needed for the formation of the complex. The calculated stability for the complex, i.e., ~ 50 meV, could be underestimated in the preliminary calculations, since the basis set used was not rich enough to reproduce charge-transfer effects between the polyyne molecule and polymeric iodine units. With an improved treatment by using an appropriate theoretical model and a larger basis set, which leads to a better evaluation for stabilization energy due to charge transfer, the nature of the bonding and the barrier for the backward reaction are to be rationalized.

A concrete picture for the polyyne-iodine complex mentioned above provides us with an implication for the formation mechanism. Absorption of a photon by an I_2 molecule leads to dissociation into two iodine atoms.³⁶ When the two iodine atoms are received by the other two I_2 molecules, a unit of I_6 can presumably be formed. Such a polymeric unit of iodine can be stabilized in the presence of a polyyne molecule in between. In other words, two I_3 units and one polyyne molecule form a stable complex.

This hypothetical mechanism is to be examined in view of the observations presented in the preceding sections. (i) Stoichiometry for the reaction being $n = 3$ indicates simultaneous consumption of three I_2 molecules per one polyyne molecule upon photo absorption. (ii) The observation of the 2-fold lines in the NMR spectra means the presence of a symmetric center. (iii) Vibronic level structures associated with the near-UV absorption spectra indicate that the skeletal polyynic carbon chain is retained. All the three issues are explainable by the formation of a weakly bound molecular complex with a polyyne and two I_3 units. In order to stabilize two iodine atoms immediately, at least three, additionally more than three, I_2 molecules are better surrounding the polyyne molecule, forming a cluster of $C_{2n}H_2(I_2)_m$ ($m \geq 3$), before photodissociation of an I_2 molecule takes place.

3.7. Electronic Transitions in $C_{2n}H_2I_6$. Finally, the reason why the appearance in the UV/vis absorption spectra changes so dramatically remains to be explained. For the centrosymmetric linear polyyne molecule in $D_{\infty h}$ point group symmetry, two types of transitions are optically allowed, i.e., $\Sigma_u^+ \leftarrow \Sigma_g^+$ with a transition dipole along the molecular axis, z , stemming from $\pi-\pi^*$ excitations and located in the UV,²⁸ and $\Pi_u \leftarrow \Sigma_g^+$ with transition dipoles perpendicular to the molecular axis, x, y , stemming from $\pi-\sigma^*$ excitations and located in the vacuum UV.³⁰ According to molecular orbital calculations, e.g., TDDFT/cc-pVDZ and CIS/cc-pVDZ for $C_{10}H_2$, there are a number of spin-singlet excited states below the one for first allowed transition, ${}^1\Sigma_u^+ \leftarrow {}^1\Sigma_g^+$, i.e., lowest two, ${}^1\Sigma_u^-$ and ${}^1\Delta_u$, are located close in energy, and some others, ${}^1\Sigma_g^-, {}^1\Delta_g, {}^1\Sigma_u^-, {}^1\Delta_u$ are in-between

the lowest two and the upper-lying ${}^1\Sigma_u^+$ state, to which the optical transition from the ground state, ${}^1\Sigma_g^+$, is fully allowed.³⁵

In the literature, the absorption bands for polyynes, $C_{2n}H_2$ ($n = 5-7$), in the near-UV region correspond to vibronic bands in the symmetry-forbidden transition of $\Delta_u \leftarrow \Sigma_g^+$ in $D_{\infty h}$.³¹ The transition is weakly allowed by the Herzberg-Teller mechanism.³⁷⁻³⁹ For $\Delta_u \leftarrow \Sigma_g^+$, the intensity can be borrowed from the fully allowed transition, $\Sigma_u^+ \leftarrow \Sigma_g^+$ or $\Pi_u \leftarrow \Sigma_g^+$, upon simultaneous activation or deactivation of trans-bending π_g mode of vibration as an inducing mode.^{18,31} For intact polyynes, intensity for the vibronically allowed transition is 2 orders of magnitude lower than that for the allowed transition.^{18,30} From close resemblance in the vibronic pattern compared in Table 1, the series of absorption features intensified in the near-UV region are associated with the vibronic bands in the forbidden transition for the lowest ${}^1\Delta_u$ state, ${}^1\Delta_u \leftarrow X^1\Sigma_g^+$. The newly appearing features in-between the allowed and the forbidden transition are tentatively ascribed to another forbidden transition to the second-lowest ${}^1\Delta_u$ state, $2^1\Delta_u \leftarrow X^1\Sigma_g^+$.

In order to activate those electronic transitions, reduction of the symmetry from $D_{\infty h}$ to D_{2h} is conceivable. The ground state of Σ_g^+ in $D_{\infty h}$ is reduced to A_g in D_{2h} . The excited states mentioned above are reduced from Σ_u^- to A_u , Δ_u to $A_u \oplus B_{1u}$, Σ_g^- to B_{1g} , and Δ_g to $A_g \oplus B_{1g}$. In the lowered symmetry in D_{2h} , transition to an excited state of B_{1u} from the ground state of A_g becomes allowed, i.e., $B_{1u} \leftrightarrow A_g$, whereas transition to an excited state of A_u is still forbidden, i.e., $A_u \nleftrightarrow A_g$. Among the possible excited states, one of the doubly degenerate states in Δ_u namely the state of B_{1u} becomes optically accessible from the ground state of A_g symmetry. On further lowering of molecular symmetry to C_{2h} , transitions to the other excited states of A_u (Σ_u^-) and $A_u \oplus B_u$ (Δ_u) are predicted to become allowed.

In the present case for polyyne-iodine complexes of $C_{2n}H_2I_6$ ($n = 5-7$), however, the forbidden bands were intensified without changing the transition energy very much. The observation indicated that the electronic, as well as vibrational, level structure, thus, the polyynic molecular frame, remained almost unchanged. Only the magnitude of the transition moment was altered. How could it be possible? Due to the overlap in molecular orbitals between the polyyne molecule and the polymeric iodine unit, the former can be excited together with the latter, leading to a dramatic enhancement in absorption intensity. Note that anionic I_3^- is known to have strong UV absorption spanning from 260 to 450 nm with an absorption coefficient on the order of $\sim 10^4 \text{ cm}^{-1} \text{ mol}^{-1}$, showing two maxima centered at ~ 290 and ~ 360 nm.⁴⁰⁻⁴² These features in the absorption spectrum of I_3^- coincided well with the spectral range for polyyne-iodine complexes, $C_{2n}H_2I_6$ ($n = 5-7$), in Figure 1. Thus, in nature, it is the transition of an electron in the polymeric iodine unit, which couples with a vibronic excitation of the polyyne molecule.

For the polyyne-iodine complex, symmetry selection rule for the polyyne molecule is not largely affected, because the observed vibronic features were identified to be the same as those weakly observable without iodine. Instead, optical absorption occurs easily by the electronic transition in the polymeric iodine moiety. Since it is close in resonance to the transition for polyyne molecules, absorption intensity for the vibronic bands in the forbidden electronic transition for centrosymmetric polyyne molecules is strongly enhanced, and thus intensified as demonstrated experimentally in Figure 1.

4. CONCLUSIONS

Photoinduced reaction for three polyyne molecules, $C_{10}H_2$, $C_{12}H_2$, $C_{14}H_2$, with iodine molecules in nonpolar solvents of hexane and TCE- d_2 was studied to find a dramatic change in the UV/vis absorption spectra. The complex-forming reaction revealed following features. (1) Stoichiometry being $n = 3$: a polyyne molecule reacts simultaneously with three I_2 molecules. (2) Photoinduced reaction: the reaction is initiated by absorption of a photon by an I_2 molecule and a total three I_2 molecules are involved. (3) Polyyne chain restored: the vibronic bands in the symmetry-forbidden transition in the near UV are intensified by the reaction with iodine, with keeping the energy-level structure as that for the intact polyyne molecule. (4) Symmetric center: the 2-fold lines in the NMR spectra indicate that the reaction products, $C_{10}H_2I_6$ and $C_{12}H_2I_6$, hold a symmetric center. The UV absorption features observed for polyyne-iodine complexes of $C_{2n}H_2I_6$ are associated with the electronic transition of the polymeric iodine system coupled with the vibronic transition of the polyyne molecule.

AUTHOR INFORMATION

Corresponding Author

*E-mail: wakaba@chem.kindai.ac.jp.

ACKNOWLEDGMENT

We thank Professor Dr. Wolfgang Krätschmer (Max-Planck-Institut für Kernphysik) and Dr. Dmitry Strel'nikov (University of Karlsruhe) for their kind arrangement of isotope-enriched carbon powder. Dr. Toshie Minematsu (Department of Pharmaceutical Sciences, Kinki University) is acknowledged for the NMR measurement. T. W. and Y. W. appreciated the support from "Open Research Center" Project for Private University subsidy from The Ministry of Education, Culture, Sports, Science, and Technology (MEXT).

REFERENCES

- Ravagnan, L.; Piseri, P.; Bruzzi, M.; Miglio, S.; Bongiorno, G.; Baserga, A.; Casari, C. S.; Li Bassi, A.; Lenardi, C.; Yamaguchi, Y.; Wakabayashi, T.; Bottani, C. E.; Milani, P. *Phys. Rev. Lett.* **2007**, *98*, 216103.
- Slepkov, A. D.; Hegmann, F. A.; Eisler, S.; Elliott, E.; Tykwinski, R. R. *J. Chem. Phys.* **2004**, *120*, 6807.
- Diederich, F.; Stang, P. J.; Tykwinski, R. R., Eds.; *Acetylene Chemistry: Chemistry, Biology, and Material Science*; Wiley-VCH: Weinheim, Germany, 2005.
- Eisler, S.; Slepkov, A. D.; Elliott, E.; Luu, T.; McDonald, R.; Hegmann, F. A.; Tykwinski, R. R. *J. Am. Chem. Soc.* **2005**, *127*, 2666.
- Lucotti, A.; Tommasini, M.; Fazzi, D.; Del Zoppo, M.; Chalifoux, W. A.; Ferguson, M. J.; Zerbi, G.; Tykwinski, R. R. *J. Am. Chem. Soc.* **2009**, *131*, 4239.
- Chalifoux, W. A.; McDonald, R.; Ferguson, M. J.; Tykwinski, R. R. *Angew. Chem., Int. Ed.* **2009**, *48*, 7915.
- Nagano, Y.; Ikoma, T.; Akiyama, K.; Tero-Kubota, S. *J. Am. Chem. Soc.* **2003**, *125*, 14103.
- Cataldo, F.; Ravagnan, L.; Cinquanta, E.; Castelli, I. E.; Manini, N.; Onida, G.; Milani, P. *J. Phys. Chem. B* **2010**, *114*, 14834.
- Sun, A.; Lauher, J. W.; Goroff, N. S. *Science* **2006**, *312*, 1030.
- Chalifoux, W. A.; Tykwinski, R. R. *Nat. Chem.* **2010**, *2*, 967.
- Ravagnan, L.; Siviero, F.; Lenardi, C.; Piseri, P.; Barborini, E.; Milani, P.; Casari, C. S.; Li Bassi, A.; Bottani, C. E. *Phys. Rev. Lett.* **2002**, *89*, 285506.
- Wakabayashi, T.; Ong, A.-L.; Strel'nikov, D.; Krätschmer, W. *J. Phys. Chem. B* **2004**, *108*, 3686.
- Tsuji, M.; Tsuji, T.; Kuboyama, S.; Yoon, S.-H.; Korai, Y.; Tsujimoto, T.; Kubo, K.; Mori, A.; Mochida, I. *Chem. Phys. Lett.* **2002**, *355*, 101.
- Cataldo, F. *Carbon* **2003**, *41*, 2653; Cataldo, F., Ed.; *Polyynes: Synthesis, Properties, and Applications*; CRC and Taylor & Francis: Boca Raton, FL, 2006.
- Inoue, K.; Matsutani, R.; Sanada, T.; Kojima, K. *Carbon* **2010**, *48*, 4209. Matsutani, R.; Ozaki, F.; Yamamoto, R.; Sanada, T.; Okada, Y.; Kojima, K. *Carbon* **2009**, *47*, 1659. Matsutani, R.; Kakimoto, T.; Wada, K.; Sanada, T.; Tanaka, H.; Kojima, K. *Carbon* **2008**, *46*, 1103.
- Tabata, H.; Fujii, M.; Hayashi, S.; Doi, T.; Wakabayashi, T. *Carbon* **2006**, *44*, 3168.
- Wakabayashi, T.; Tabata, H.; Doi, T.; Nagayama, H.; Okuda, K.; Umeda, R.; Hisaki, I.; Sonoda, M.; Tobe, Y.; Minematsu, T.; Hashimoto, K.; Hayashi, S. *Chem. Phys. Lett.* **2007**, *433*, 296.
- Wakabayashi, T.; Nagayama, H.; Daigoku, K.; Kiyooka, Y.; Hashimoto, K. *Chem. Phys. Lett.* **2007**, *446*, 65.
- Nishide, D.; Dohi, H.; Wakabayashi, T.; Nishibori, E.; Aoyagi, S.; Ishida, M.; Kikuchi, S.; Kitaura, R.; Sugai, T.; Sakata, M.; Shinohara, H. *Chem. Phys. Lett.* **2006**, *428*, 356.
- Nishide, D.; Wakabayashi, T.; Sugai, T.; Kitaura, R.; Kataura, H.; Achiba, Y.; Shinohara, H. *J. Phys. Chem. C* **2007**, *111*, 5178.
- Malard, L. M.; Nishide, D.; Dias, L. G.; Capaz, R. B.; Gomes, A. P.; Jorio, A.; Achete, C. A.; Saito, R.; Achiba, Y.; Shinohara, H.; Pimenta, M. A. *Phys. Rev. B* **2007**, *76*, 233412.
- Moura, L. G.; Malard, L. M.; Carneiro, M. A.; Venezuela, P.; Capaz, R. B.; Nishide, D.; Achiba, Y.; Shinohara, H.; Pimenta, M. A. *Phys. Rev. B* **2009**, *80*, 161401(R).
- Wakabayashi, T.; Murakami, T.; Nagayama, H.; Nishide, D.; Kataura, H.; Achiba, Y.; Tabata, H.; Hayashi, S.; Shinohara, H. *Eur. Phys. J. D* **2009**, *52*, 79.
- Benesi, H. A.; Hildebrand, J. H. *J. Am. Chem. Soc.* **1949**, *71*, 2703.
- Cheng, P. Y.; Zhong, D.; Zewail, A. H. *J. Chem. Phys.* **1996**, *105*, 6216.
- DeBoer, G.; Burnett, J. W.; Fujimoto, A.; Young, M. A. *J. Phys. Chem.* **1996**, *100*, 14882.
- Kiviniemi, T.; Hulkko, E.; Kiljunen, T.; Pettersson, M. *J. Phys. Chem. A* **2009**, *113*, 6326.
- Eastmond, R.; Johnson, T. R.; Walton, D. R. M. *Tetrahedron* **1972**, *28*, 4601.
- Pino, T.; Ding, H.; Güthe, F.; Maier, J. P. *J. Chem. Phys.* **2001**, *114*, 2208.
- Kloster-Jensen, E.; Haink, H.-J.; Christen, H. *Helv. Chim. Acta* **1974**, *57*, 1731.
- Ding, H.; Schmidt, T. W.; Pino, T.; Güthe, F.; Maier, J. P. *Phys. Chem. Chem. Phys.* **2003**, *5*, 4772.
- Gao, K.; Goroff, N. S. *J. Am. Chem. Soc.* **2000**, *122*, 9320.
- Webb, J. A.; Liu, P.-H.; Malkina, O. L.; Goroff, N. S. *Angew. Chem., Int. Ed.* **2002**, *41*, 3011.
- Schermann, G.; Grösser, T.; Hampel, F.; Hirsch, A. *Chem.—Eur. J.* **1997**, *3*, 1105.
- Frisch, M. J. et al. *Gaussian 03*, revision E.01; Gaussian Inc.: Wallingford, CT, 2004.
- Herzberg, G.; *Molecular Spectra and Molecular Structure: Spectra of Diatomic Molecules*, 2nd ed.; Van Nostrand: New York, 1950.
- Orlandi, G.; Siebrand, W. *J. Chem. Phys.* **1973**, *58*, 4513.
- Lin, S. H.; Eyring, H. *Proc. Natl. Acad. Sci. U.S.A.* **1974**, *71*, 3415.
- Lin, S. H.; Eyring, H. *Proc. Natl. Acad. Sci. U.S.A.* **1974**, *71*, 3802.
- Ashkenazi, G.; Banin, U.; Bartana, A.; Kosloff, R.; Ruhman, S. *Adv. Chem. Phys.* **1997**, *100*, 229.
- Choi, H.; Bise, R. T.; Hoops, A. A.; Neumark, D. M. *J. Chem. Phys.* **2000**, *113*, 2255.
- Kerenskaya, G.; Goldschleger, I. U.; Apkarian, V. A.; Fleischer, E.; Janda, K. C. *J. Phys. Chem. A* **2007**, *111*, 10969.